

Supporting Information

Towards controlled photothermal treatment of single cell: Optically induced heating and remote temperature monitoring in-vitro through double wavelength optical tweezers

Sławomir Drobczyński^{†,}, Katarzyna Prorok[⊥], Konstantin Tamarov[§], Kamila Duś-Szachniewicz^{||},
Vesa-Pekka Lehto[§], Artur Bednarkiewicz^{⊥,#,*}*

[†]Department of Optics and Photonics, Wrocław University of Technology, Wybrzeże Stanisława Wyspiańskiego 27, 50-370 Wrocław, Poland

[⊥] Wrocław Research Center EIT+, Stabłowicka 147, 54-066 Wrocław, Poland

[§] Department of Applied Physics, University of Eastern Finland, 70211, Kuopio, Finland

^{||} Department of Pathology, Wrocław Medical University, Marcinkowskiego 1, 50-368 Wrocław, Poland

[#] Institute of Low Temperature and Structure Research of the Polish Academy of Sciences, Okólna 2, 50-422 Wrocław, Poland

Upconverting Nanoparticles Synthesis

Yttrium oxide (99.99%), ytterbium oxide (99.99%), and erbium oxide (99.99%) acetic acid (99%), pure oleic acid and 1-octadecene (90%) were purchased from ALDRICH Chemistry. Ethanol (96% pure p.a.), n-hexane (95%) and acetone (pure p.a.) and chloroform were purchased from POCH S.A. (Poland). All the chemical reagents were used as received without future purification.

Stoichiometric amounts of respective Er_2O_3 , Yb_2O_3 , and Y_2O_3 lanthanide oxides were mixed with 50% aqueous acetic acid. The mixture was stirred and heated up to obtain a clear and transparent solution. The final precursor was obtained by evaporation of solvents and further drying at 130°C for 24h.

Synthesis of core nanoparticles

The lanthanide acetate— $(\text{CH}_3\text{COO})_3\text{Y}$, $(\text{CH}_3\text{COO})_3\text{Yb}$ and $(\text{CH}_3\text{COO})_3\text{Er}$ — 2.5 mmol were added to the flask with 15 ml oleic acid and 38 ml octadecene. The solution was stirred and heated up to 140°C under vacuum for 30 min in order to form the $\text{Ln}(\text{oleate})_3$ complex (where Ln stands for Y, Yb or Er) and to remove total oxygen and remaining water. Next, the temperature was lowered to 50°C and 10 mmol ammonium fluoride (NH_4F) and 6.25 mmol sodium hydroxide (NaOH) dissolved in 20 ml of methanol were added to the reaction flask. The resulting cloudy mixture was stirred for 30 minutes at 70°C . Next, the reaction temperature was increased and the methanol was evaporated. After removing methanol, the solution was heated up to 300°C under a nitrogen atmosphere and maintained under these conditions for 1 hour. Next, the nanoparticles

were precipitated using acetone and n-hexane, centrifuged at 10000 rpm for 10 min and washed with ethanol. Finally, the prepared core NPs were dispersed in chloroform.

Synthesis of core/shell nanoparticles

The yttrium acetate (2.5 mmol) was added to the flask with 15 ml oleic acid and 38 ml octadecene. The solution was stirred and heated up to 140°C under vacuum for 30 min to form the Y(oleate)₃ complex and to remove total oxygen and remaining water. The temperature was lowered to 60°C and the reaction flask was placed under a flow of nitrogen. A solution of core nanoparticles in CHCl₃ was added to the solution. The solution was maintained at 80°C until all the chloroform was removed. Next, the temperature was lowered to 50°C and 10 mmol ammonium fluoride (NH₄F) and 6.25 mmol sodium hydroxide (NaOH) dissolved in 20 ml of methanol were added to the reaction flask. The resulting cloudy mixture was stirred for 30 minutes at 70°C. Next, the reaction temperature was increased and the methanol was evaporated. After methanol removal, the solution was heated up to 300°C under a nitrogen atmosphere and held in these conditions for 1 hour. Next, the nanoparticles were precipitated using acetone and n-hexane, centrifuged at 10000 rpm for 10 min and washed with ethanol. Finally, the prepared nanoparticles were dispersed in chloroform.

Silica microspheres

In a typical experiment, approximately 1.5 g of compressed yeast were suspended in 3 ml of solvents (1 ml H₂O + 2 ml ethanol). A solution of core/shell nanoparticles in CHCl₃ (1 ml) was added to the solution. After the addition of 0.25 ml of ammonia as a catalyst and 2.5 ml of TEOS, the suspension was agitated at room temperature for 24 h. The product was recovered by

centrifugation (5 min at 4000 rpm) and washed twice with alcohol following a washing step with water. Afterwards, the precipitate was dried at 105°C to constant weight.

Porous silicon microparticles (Si μ Ps)

To obtain the PSi MPs, 10 cm crystalline Si wafers (orientation of 100, the resistivity of 0.01 - 0.02 $\Omega\cdot\text{cm}$) were etched in 1:1 HF:EtOH electrolyte at 50 mA/cm² for 40 minutes. Then the detached PSi layer was dried at 65°C, milled with a planetary ball mill and sieved to 53-75 μm fraction first by dry sieving and then by wet sieving with EtOH. The average pore size of 30 nm for UCNPs loading was obtained by annealing for 45 minutes at 625°C in a nitrogen atmosphere. Finally, the PSi MPs were oxidized at 300°C in air to make them hydrophilic.

Cells

Diffuse Large B-cell Lymphoma cell line SU-DHL-10 was purchased from ATCC (American Type Culture Collection, Manassas, VA, USA). Cells were cultured in RPMI-1640 medium (ATCC) supplemented with heat inactivated 10% (v/v) fetal bovine serum (FBS) (Gibco, Thermo Fisher Scientific, Waltham, MA, USA) at 37°C in 5% CO₂ in a humidified incubator. The cultures were maintained by addition of fresh medium or replacement of medium every 2-3 days. When the cell concentration reached 2×10^6 viable cells/mL, subsequent cultures were established by centrifugation followed by resuspension in fresh medium at 5×10^5 viable cells/mL.

The Trypan Blue Solution, 0.4% (Thermo Fischer Scientific, Darmstadt, Germany) was added to the cell suspension in order to determine the viability of the monitored cell. This test relies on the fact that living cells possess intact cell membranes that exclude Trypan Blue (TB) dye, a

property no longer present in dead cells. As a consequence, viable cells display a transparent cytoplasm, whereas nonviable cells become dark owing to the accumulation of TB within the cytoplasm of the cell. In our study, a cell suspension was mixed with dye and visually examined in order to provide information about temperature-induced death.

Upconverting nanoparticles

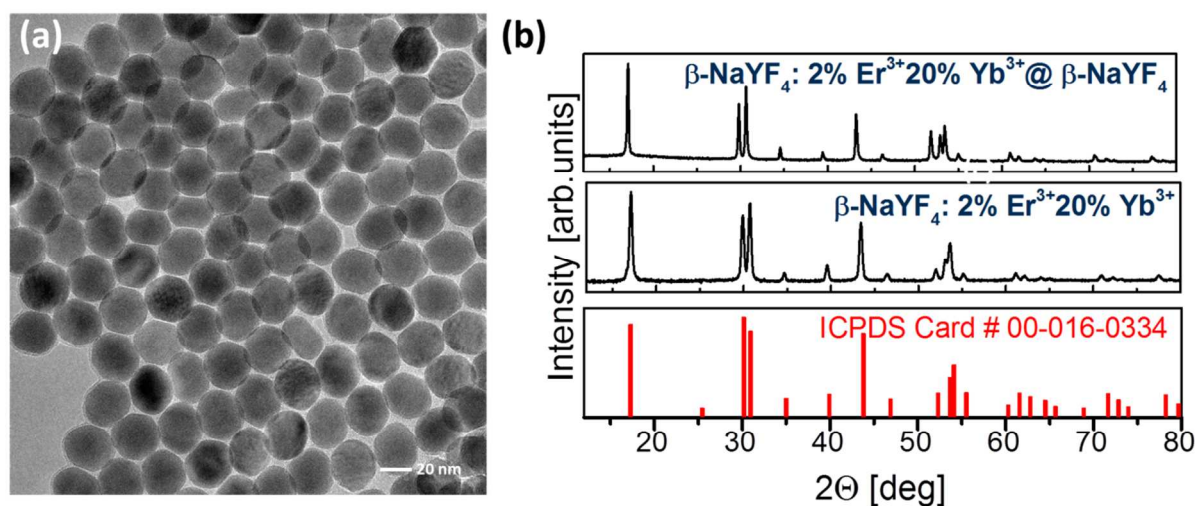


Figure S1. TEM image of the $\text{NaYF}_4:\text{Er}^{3+}, \text{Yb}^{3+} @ \text{NaYF}_4$ core@shell nanoparticles. (b) The XRD pattern of core and core@shell nanoparticles is evidence of the phase pure hexagonal nanomaterials with a narrow size distribution.

Silicon microparticles as heaters

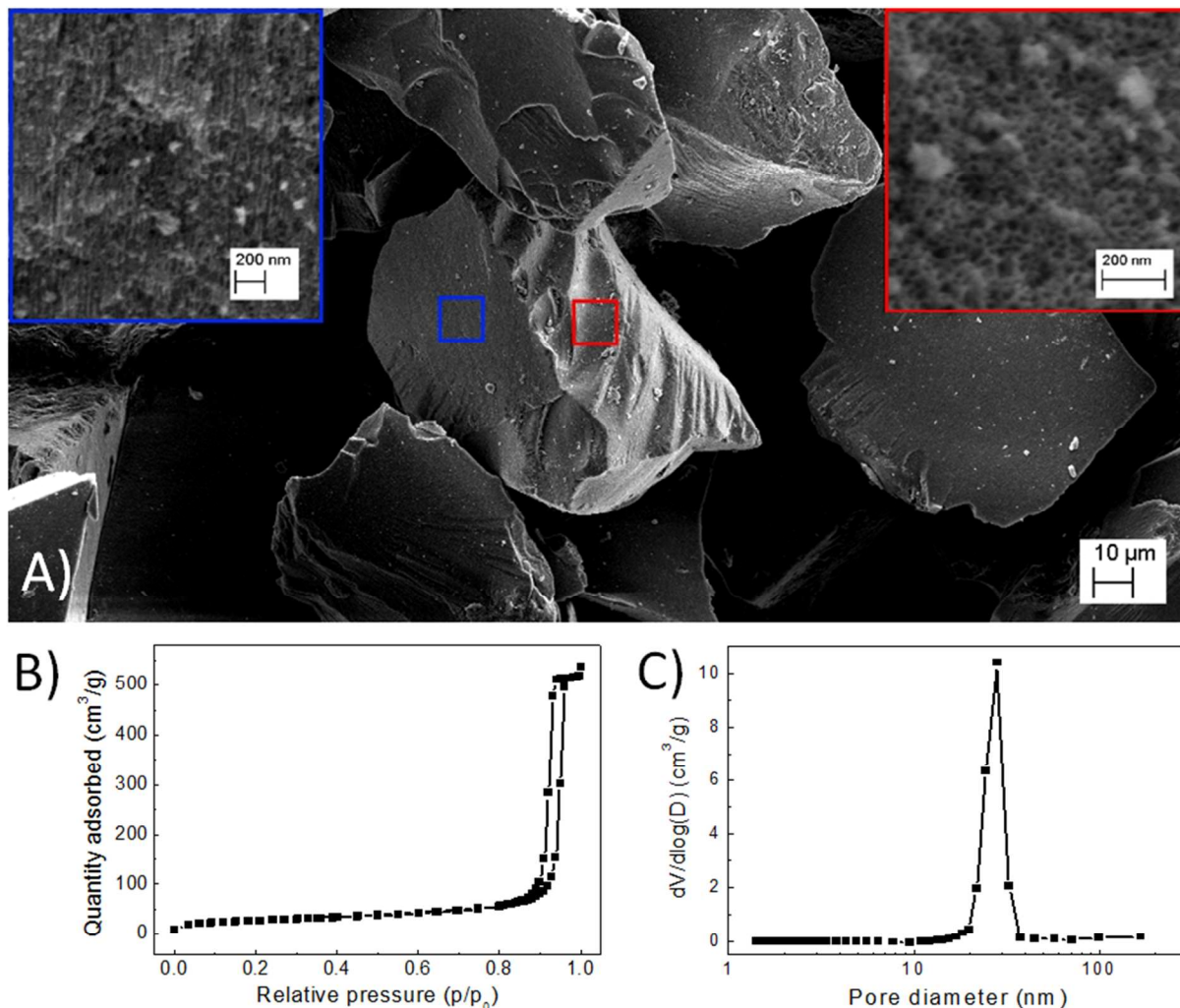


Figure S2. Structural properties of SiμPs: (a) SEM image of SiμPs; the insets show the pore morphology from different planes; (b) N₂ adsorption-desorption isotherms and (c) pore size distribution of SiμPs.

To obtain the SiμPs, 10 cm crystalline Si wafers (orientation of 100, resistivity of 0.01 - 0.02 Ω·cm) were etched in 1:1 HF:EtOH electrolyte at 50 mA/cm² for 40 minutes. Then the detached porous silicon layer was dried at 65°C, milled in a planetary ball mill and sieved to 53-75 μm fraction first by dry sieving and then by wet sieving with EtOH.^[1] The average pore size

of 30 nm for UCNPs loading was obtained by annealing for 45 minutes at 625°C in an N₂ atmosphere.^[2] Finally, the SiμPs were oxidized at 300°C in air to make them hydrophilic. SiμPs were imaged with scanning electron microscopy (Zeiss Sigma HD|VP) and the pore sizes and volumes were determined with N₂ adsorption/desorption (Micrometrics Tristar II). Figure S2 shows the SEM images of SiμPs and the pore size distribution. The average pore diameter was 20 nm and the cumulative pore volume was 0.8 cm³/g.

Optical setup

Four different ways of trap generation at two different wavelengths have been verified in our laboratory, namely (i) simultaneous traps generation using GMXY and SLM lasers operating using a continuous wave beam, (ii) traps control by GMXY, (iii) traps control using the SLM working with pulse lasers, (iv) traps generation using the SLM with continuously operating lasers.

In the first embodiment, simultaneous traps were generated by using GMXY and SLM systems and lasers operating in a continuous wave mode. The beam of Nd:YAG laser at 1064 nm was directed to the *Laser port1*, and the beam position was controlled by GMXY. The collimated beam from pigtailed laser diode 980 nm was directed to a *Laser port2* to illuminate the SLM modulator. The two lenses *L1* and *L2* extended the laser beam and the telescope composed of *L3* and *L5* lenses overfilled the back aperture of high NA objective. The low-pass dichroic mirror *DMI* ($\lambda_{\text{edge}} = 1000$ nm) was used. The transmission of the respective optical elements in NIR range was equal to ~100%, ~90% and ~50% for the DMSP805R filter, the DMSP10000R filter and the microscope objective, respectively. The telescope consisted of *L4* and *L5* lenses in $4f$ transferred the plane of the SLM to the Fourier plane of the high NA microscope objective. The

objective was responsible for strong focusing of the beam being diffracted on the CGH structure (displayed on the SLM) and actual forming the optical traps.

In the second approach, traps were controlled by the GMXY system. Nd: YAG laser and pigtailed laser diode were used as the inputs of single mode fiber coupler (SMFC), whose output was directed to *Laser port1*. Beam modulation of both lasers was computer controlled. The inclusion of a fiber coupler was advantageous because it made it possible to undertake the axial operation of both laser beams, which enabled replacing dichroic mirrors *DMI*, by an aluminum flat mirror reflecting two laser beams. The generation of two wavelength traps by GMXY was based on a time sharing method ^[3]. The basic principle behind the generation of a trap of a given wavelength at a given position relies on sequential positioning and simultaneously synchronized switching the individual laser beams (either 1064 nm or 980nm) on/off.

Another approach utilized was similar to the previous setup, but instead of GMXY, the SLM was working in time sharing mode to generate and control traps. The collimated laser beam from CLS was introduced to *Laser port 2* and illuminated the SLM modulator. In this setup, the dichroic mirror *DMI* was removed. The SLM modulator was displaying holograms dedicated to the 980nm and 1064nm beams in an alternated and synchronous manner. At the same time, the appropriate lasers were synchronously switched on/off. The laser pulses were synchronized to the refresh screen synchronization using the signal generated by the graphics card. The real-time hologram calculation was performed using the NVIDIA CUDA, while the calculated phase maps were displayed on the SLM modulator using DirectX, which enabled interception of screen refresh synchronization signal. The whole measurement system was controlled by a program developed in-house using C ++ \ CLI for .NET.

In the last approach, the traps were generated and controlled using the SLM with continuously operating lasers. The system configuration described in the previous setup was supplemented with a bipartite filter placed in front of the SLM. One-half of this filter was transparent for the 980 nm laser, while the other half was transparent for the 1064nm beam. This kind of filter made it possible to illuminate one-half of SLM with a 980 nm beam and the other half with the 1064 nm beam. An example hologram is shown in Figure S3b.

All of the described setups had their own advantages and disadvantages. For example with the first setup, both GMXY and SLM laser sources could work in the continuous mode, which provided high optical power (suitable for heating the sample). The SLM was suitable for performing the XYZ-translation of the thermometers and precisely adjust the system to improve S/D luminescence collection as well as requiring fewer traps (sharing the power) and Laguerre-Gauss beams. Because there are two separate optical systems involved, the alignment and overlapping beams was somewhat challenging. In the second setup, the beams share the optical path of laser excitation (pulsed mode of operation) which simplified their operation and adjustment, but only Gauss beams and Z positioning with microscope objective were feasible. The third setup also exploited shared optical paths with the shared SLM with laser beams being switched. This allowed full SML resolution, the relatively high optical power of the traps (limited by pulse width modulation depth), independent Z positioning as well as creating both Gauss and Laguerre-Gauss beams. In the last setup, only half of the SLM resolution was being used, but the lasers were working in the CW mode and shared the optical path. One advantage of this approach was that it allowed independent Z positioning and meant that both Gauss and Laguerre-Gauss beams could be utilized in the same system.

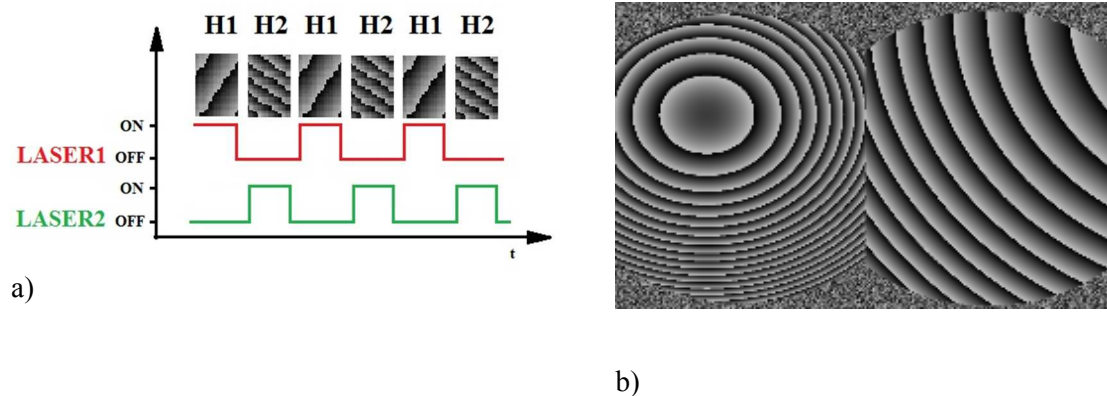


Figure S3. a - SLM time sharing mode, b – divided hologram, the left - side for 980 nm, right side for 1064 nm.

High-efficiency phase holograms were calculated using NVIDIA CUDA technology, which allowed simultaneous generation of several traps for concurrent trapping and excitation of UCNPs as well as manipulation of other elements in the sample. The use of HOT made it possible to eliminate mechanical movements of the microscopic stage and guaranteed a mechanically vibration-free method for precise positioning of the optical nano-thermometer for local temperature measurement in microscopic volumes.

Control experiments

Negative control experiments have been performed and are presented in Figure S4 to demonstrate that the cell death occurred in response to excessive heating and not due to any chemical interaction with Si μ P (Figure S4c) or O μ T (Figure S4b) particles, nor was cell damage attributable to the trapping forces and laser beams with either 980 nm (Figure S4a) or 1064 nm (Figure S4b), and furthermore, it was not influenced by the temperature readout from O μ T and (unheated) Si μ P (Figure S4d). The intensity of the optical traps was identical to the major

‘positive’ experiments. The figures present different time stamps, i.e. immediately (1st column), around 60 second (2nd column) and over 100 seconds (3rd column) after the beginning of the experimental procedure. These time points correspond to the time points presented in Figure 5. No traces of Trypan Blue accumulation were found during the whole observation time (up to 5 minutes), evidence that no cell death had occurred in any of the cases, unless the intentional localized overheating of the cell had been triggered.

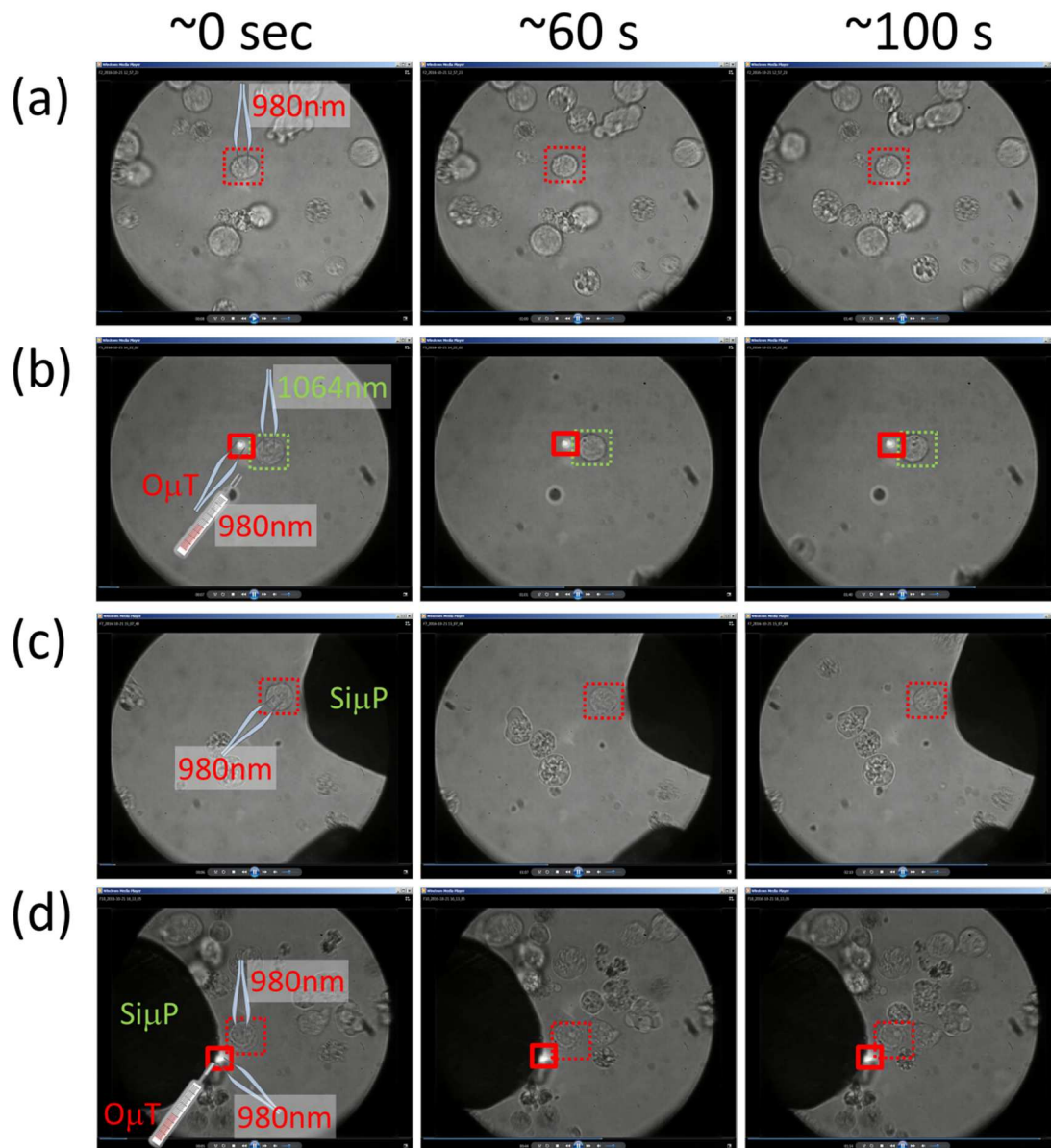


Figure S4. The negative control experiments reveal no evidence of any cell death in response to (a) trapping the cell with 980nm, (b) trapping the cell with 1064 nm trap and trapping O μ T with 980 nm trap, (c) trapping of the cell with 980 nm in close proximity to Si μ P (unheated), (d) trapping the cell with the 980 nm trap in close proximity to the O μ T trapped at 980nm and Si μ P (unheated). The images show a lack of TB accumulation at 0, ~60 and ~100 seconds after the beginning of these above experiments, which correspond in time to the major experiment (Figure 5). No signs of TB accumulation were observed during much longer (a few minutes) observation times.

References

- [1] H. A. Santos, J. Riikonen, J. Salonen, E. Mäkilä, T. Heikkilä, T. Laaksonen, L. Peltonen, V.-P. Lehto, J. Hirvonen, *Acta Biomater.* **2010**, 6, 2721.
- [2] J. Salonen, E. Mäkilä, J. Riikonen, T. Heikkilä, V.-P. Lehto, *Phys. Status Solid.* **2009**. 6, 1313.
- [3] M. Capitano, R. Cicchi R, F.S Pavone, *Opt. Lasers Eng.* **2007**, 45, 450.